Electronic suplementary information (ESI) for:

How can $[Mo^{IV}(CN)_6]^{2-}$, an apparently octahedral $(d)^2$ complex, be diamagnetic? Insights from quantum chemical calculations and magnetic susceptibility measurements.

Mariusz Radoń*, Paweł Rejmak, Magdalena Fitta,

Maria Bałanda, and Janusz Szklarzewicz*

List of Tables

List of Figures

Other supporting materials

(provided as separate files)

- Pseudopotentials used in periodic DFT calculations and computationally optimized crystal structures.
- Animated movies of IRC paths and MD trajectories.

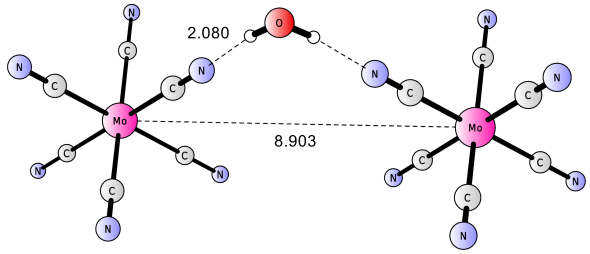

Figure S1: Structure of the two-center model $[Mo(CN)_6]^{2-}\cdots H_2O\cdots[Mo(CN)_6]^{2-}$ used to estimate the magnetic coupling between the neighboring Mo centers in the crystal structure of **1**. Atomic coordinates are based on the crystal structure (except for H atoms in the water moleculewhich were adjusted as explained in the main article) and can be found in Table S18. Annotated numbers are the CN···HO and Mo···Mo distances in Å.

Table S1: Relative energy (kcal/mol) of spin states of the two-center model.[a]

	Total spin state	
	$S_{tot} = 0$ (↑↓ coupling)	$S_{tot} = 2$ (↑↑ coupling)
BP86/def2-SV(P)	0.10	0.00
B3LYP/def2-SV(P)	0.11	0.00
B3LYP/(ma)-TZVPP[b]	0.04	0.00

[a]The model is shown in Figure S1. The considered spin states are obtained by antiparallel (↑↓, singlet) or parallel (↑↑, quintet) coupling of the two $S_1 = S_2 = 1$ spins, one on each Mo center. The spin-unrestricted results for the singlet state are not corrected for spin contamination, but since the quintet is below the singlet from the beginiing, the correction is expected to further raise the singlet up in energy. [b]def2-TZVPP (for Mo,H) or ma-TZVPP (for C,N,O).

Table S2: Calculated[a] and experimental structural parameters of $[Mo(CN)_6]^{2-}$.

	Octahedral	Trigonal prismatic
	Singlet (spin-restricted)	
Symmetry	D_{4h}	D_{3h}
Energy min.	no	yes
Imag. freq.(cm^{-1})	$i250\,(b_{2u})$	–
	$i215\,(a_{2u})$	
	$i96\,(e_u)$	
Mo−C (Å)	2.131(×2), 2.172	2.103
C−N(Å)	1.181(×2), 1.175	1.177
	Singlet (spin-unrestricted)	
Symmetry	D_{4h}	C_s
Energy min.	no	yes
Imag. freq.(cm^{-1})	$i157\,(e_u)$	–
Mo−C (Å)	2.155(×2), 2.152	2.096, 2.125, 2.126
C−N (Å)	1.177	1.176
	Triplet	
Symmetry	D_{4h}	C_{2v}
Energy min.	no	yes
Imag. freq. (cm^{-1})	$i156\,(e_u)$	–
Mo−C (Å)	2.160(×2), 2.161	2.151(×2), 2.092
C−N (Å)	1.177(×2), 1.176	1.175(×2), 1.176
	Crystal structure of **1**	
Symmetry	O_h	
Mo−C (Å)	2.090	
C−N (Å)	1.137	

[a]DFT:BP86/def2-TZVP level.

Table S3: Singlet–triplet relative energy (kcal/mol) for the octahedral geometry of $[Mo(CN)_6]^{2-}$, either the experimental one or the one optimized at the DFT level (for each spin state separately) under the D_{2h} symmetry constraints to keep it (approximately) octahedral.

	exptl	optimized under D_{2h}
PBE0	15.8	14.8
B3LYP	14.0	12.8
BP86	12.4	11.8
PBE	12.2	11.5

Table S4: Energy gain (kcal/mol) from the distortion of octahedral to trigonal prismatic structure of $[Mo(CN)_6]^{2-}$ in the triplet state.[a]

	ΔE
B3LYP	7.3
B3LYP*	8.5
OLYP	12.9
BP86	12.3
PBE	13.5
B2PLYP	9.0
CCSD(T)[b]	8.0
CASPT2[c]	12.1

[a]The octahedral structure is the one optimized at the DFT level under the D_{2h} symmetry constraints. [b]For DFT:BP86 structures and basis set (B). [c](6,7) active space, ANO-I basis, IPEA=0.25.

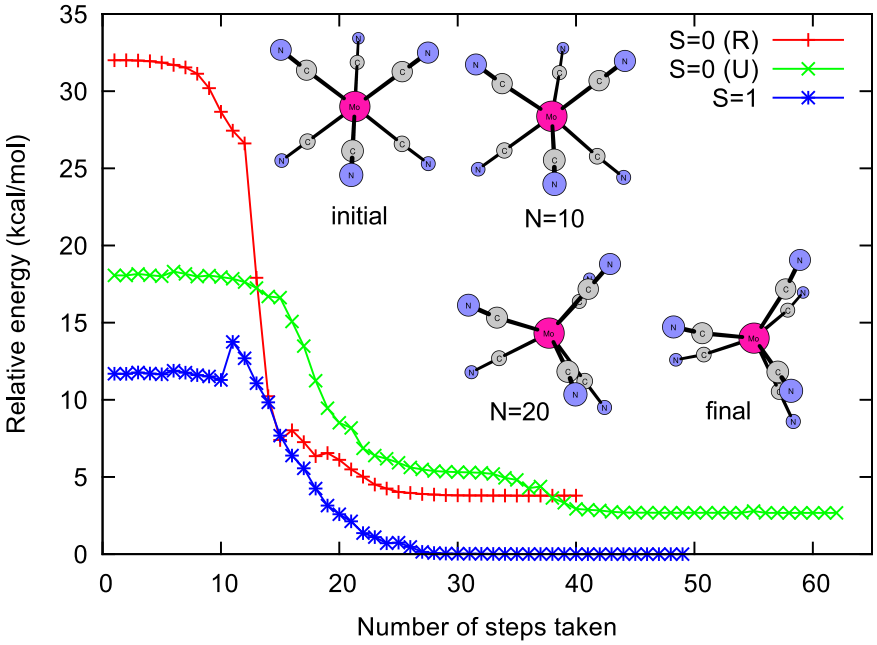

Figure S2: Energy profile of symmetry-unconstrained geometry optimizations for singlet and triplet states of $[\mathrm{Mo(CN)_6}]^{2-}$, and selected structures for the triplet state. The singlet state is taken either from restricted (R) or unrestricted (U) calculations; note that energy shown in this plot is *not* corrected for spin contamination. The initial point of each optimization is the octahedral geometry of D_{4h} symmetry (technically, optimized under the D_{2h} symmetry constraints) slightly distorted along the imaginary-frequency mode of e_u symmetry to move out the system from the unstable stationary point. The initial distortion (corresponding to $T = 1$ K) was done with `screwer` utility from the `Turbomole` suite.

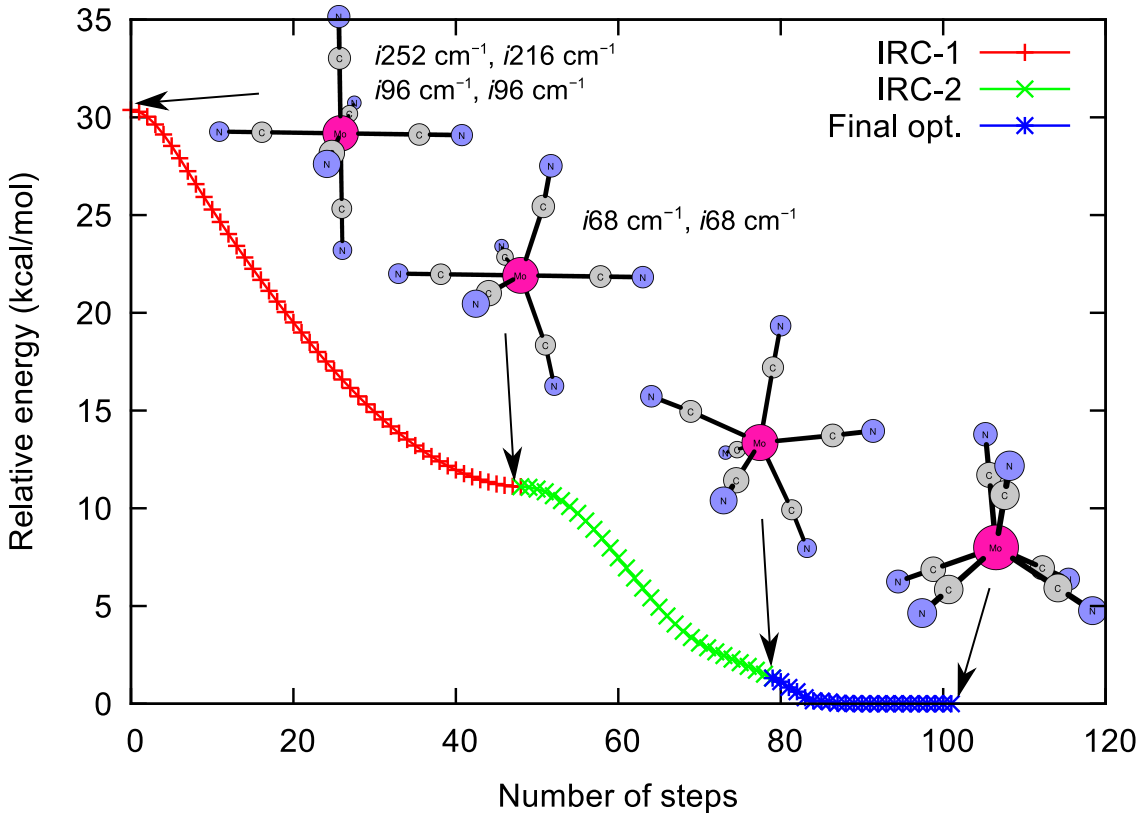

Figure S3: Energy profile at the DFT:BP86/def2-TZVP level along the reaction coordinate transforming the octahedral to the trigonal prismatic form of $[Mo(CN)_6]^{2-}$ in the singlet state ($S = 0$) from *spin-restricted* calculations. Shown are two consecutive IRC pathways (IRC-1, IRC-2) and the final geometry optimization starting from the end point of IRC-2. **Animated visualization is available as a separate movie file.**

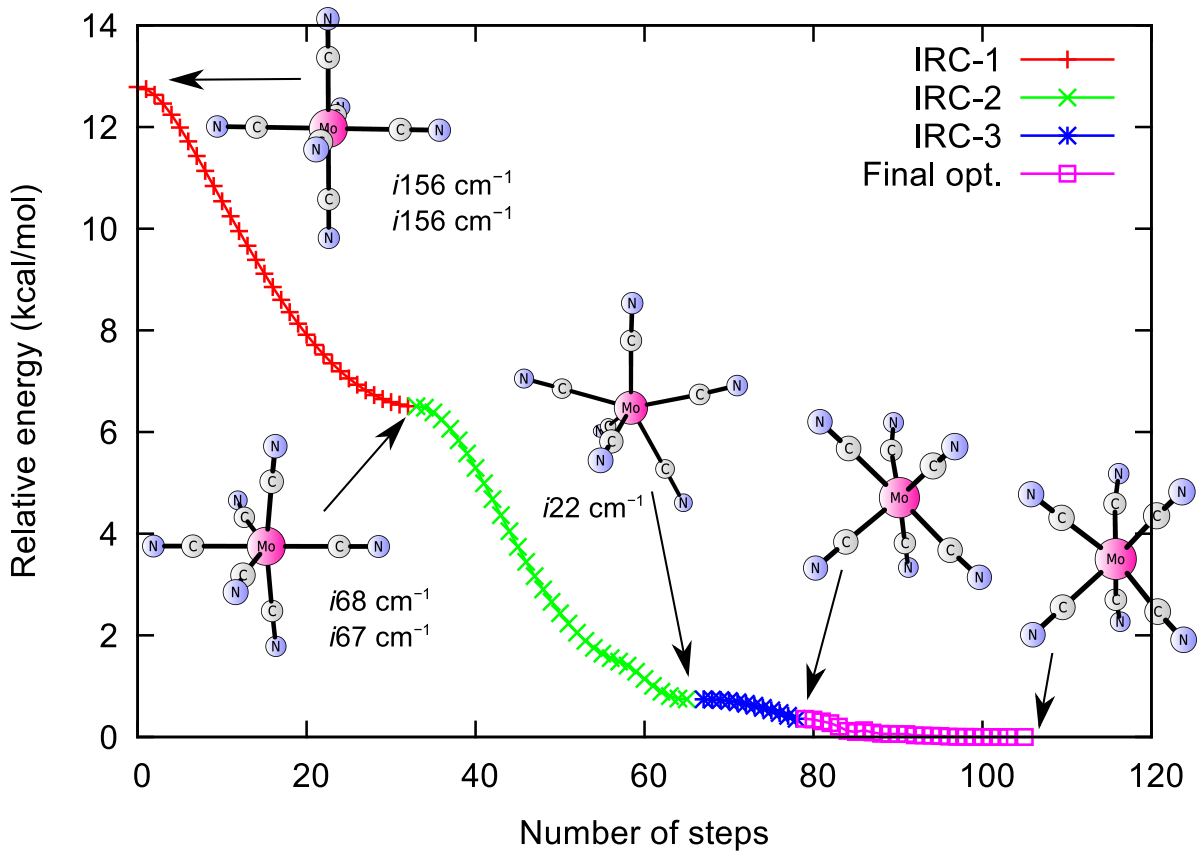

Figure S4: Energy profile at the DFT:BP86/def2-TZVP level along the reaction coordinate transforming the octahedral to the trigonal prismatic form of $[Mo(CN)_6]^{2-}$ in the single state ($S = 0$) from *spin-unrestricted* calculations. Shown are three consecutive IRC pathways (IRC-1, IRC-2, IRC-3) and the final geometry optimization starting from the end point of IRC-3. **Animated visualization is available as a separate movie file.**

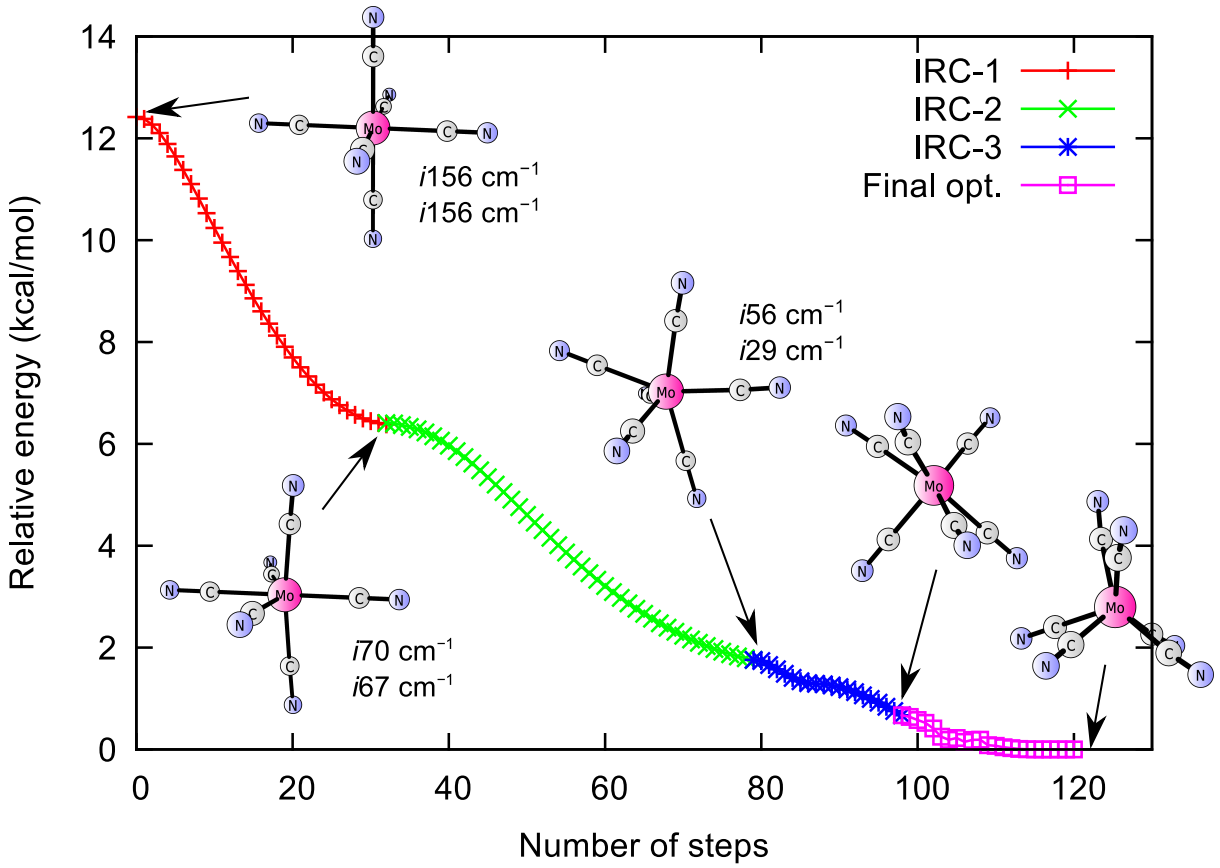

Figure S5: Energy profile at the DFT:BP86/def2-TZVP level along the reaction coordinate transforming the octahedral to the trigonal prismatic form of $[Mo(CN)_6]^{2-}$ in the triplet state ($S = 1$). Shown are three consecutive IRC pathways (IRC-1, IRC-2, IRC-3) and the final geometry optimization starting from the end point of IRC-3. **Animated visualization is available as a separate movie file.**

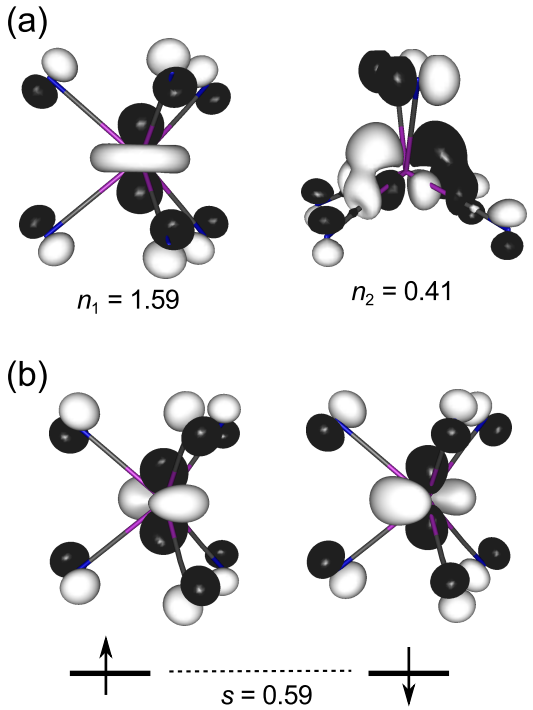

Figure S6: Contour plots of fractionally occupied natural orbitals (a) and corresponding orbitals (b) from unrestricted DFT:BP86 calculations for the open-shell singlet state; contour value ±0.04 (a.u.); natural orbitals occupations and an overlap integral between the corresponding orbitals are annotated.

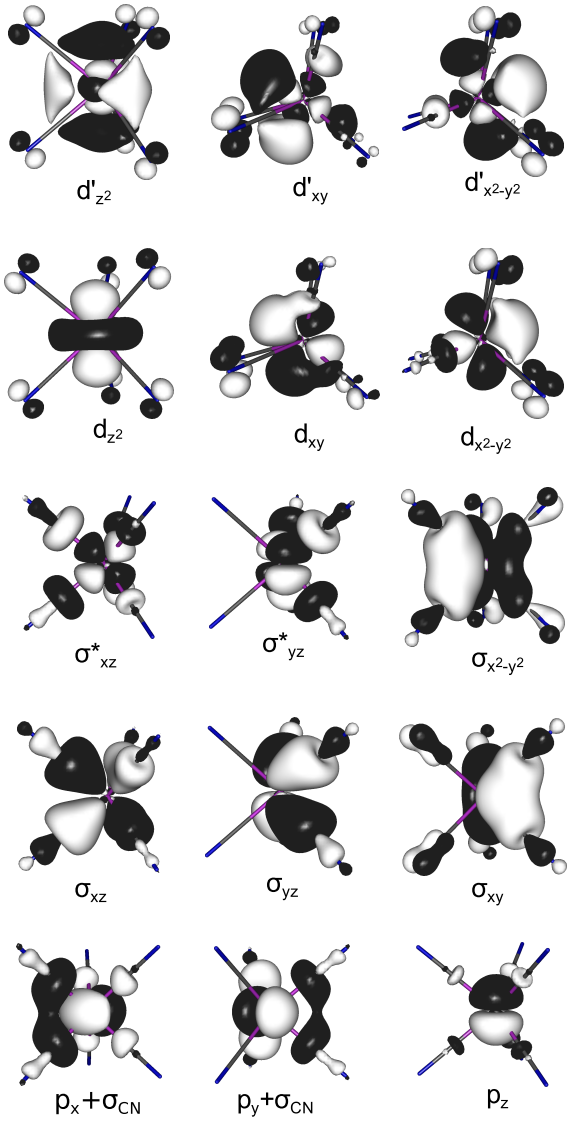

Figure S7: Contour plots of the CASSCF (16,15) active orbitals – average orbitals for the 6 singlet states originating from the $(a_1', e')^2$ configuration; contour value ± 0.04 (a.u.)

Table S5: Composition of the lowest singlet root in CASSCF calculations for the D_{3h} trigonal prismatic structure of the singlet state.

Configuration	Weight (%)
$(a'_{1,z^2})^2(e'_{xy})^0(e'_{x^2-y^2})^0$	89.1
$(a'_{1,z^2})^0(e'_{xy})^2(e'_{x^2-y^2})^0$	2.8
$(a'_{1,z^2})^0(e'_{xy})^0(e'_{x^2-y^2})^2$	2.8
Remaining	5.3

Table S6: Occupation numbers of selected natural orbitals in the lowest singlet state obtained from CASSCF and unrestricted DFT calculations (U-DFT).

	a'_1	e'	
	d_{z^2}	d_{xy}	$d_{x^2-y^2}$
CASSCF	1.868	0.075	0.075
Unrestricted DFT	1.593	0.407	0[a]

[a]Because the wave function in U-DFT is a single determinant, natural orbitals appear in pairs for which a sum of the fractional occupation numbers equals 2 (e.g., 1.593+0.407).

Table S7: Free energy correction (kcal/mol) to the relative spin-state energetics of $[Mo(CN)_6]^{2-}$ based on harmonic frequencies; the singlet state comes from either spin-restricted (SR) or spin-unrestricted (SU) calculations.[a]

T (K)	$\Delta G_{\mathrm{S-T}}$	
	SR	SU
0	0.4	0.0
100	0.6	0.2
200	0.9	0.4
300	1.1	0.6
400	1.6	1.1
500	2.0	1.5
600	2.5	1.9

[a]i.e., $\Delta G_{\mathrm{S-T}} = G_{\mathrm{S}} - G_{\mathrm{T}} = \Delta E^{ZPE}_{\mathrm{S-T}} - RT\ln\left(Q^{\mathrm{vib}}_{\mathrm{S}}/Q^{\mathrm{vib}}_{\mathrm{T}}\right) + +RT\ln(3)$.

Table S8: Relative energies (kcal/mol) of spin-orbit free and spin-orbit coupled states for the experimental octahedral geometry of $[Mo(CN)_6]^{2-}$, computed using the multi-state CASSCF/CASPT2 + RASSI approach, ANO-I basis, $\varepsilon_{\mathrm{IPEA}} = 0.25$ a.u.[a]

Term (O_h)	Spin-Orbit Free	Spin-Orbit Coupled
$^3T_{1g}$	0.0	−1.1
	0.0	−1.1
	0.0	−1.1
		−1.1
		−1.1
		1.0
		1.0
		1.0
		1.9
$^1T_{2g}$	14.5	14.6
	14.5	14.6
	14.5	14.6
^1E_g	14.6	14.7
	15.6	15.7
$^1A_{2g}$	39.7	39.9

Table S9: Relative energies (kcal/mol) of spin-orbit free and spin-orbit coupled states for the DFT-optimized trigonal prismatic structure of the spin-restricted singlet state (D_{3h} symmetry), computed using the multi-state CASSCF/CASPT2 + RASSI approach, ANO-I basis, $\varepsilon_{\mathrm{IPEA}} = 0.25$ a.u.

Term (D_{3h})	Spin-Orbit Free	Spin-Orbit Coupled
$1^1A_1'$	0.0	0.0
$^3E'$	2.4	1.3
	2.4	1.3
		2.3
		2.3
		3.4
		3.4
$1^1E'$	16.5	16.6
	16.7	16.8
$^3A_2'$	33.5	33.2
		33.5
		33.5
$2^1E'$	41.9	41.9
	42.1	42.1
$2^1A_1'$	53.6	53.8

Table S10: Relative energies (kcal/mol) of spin-orbit free and spin-orbit coupled states for the DFT-optimized trigonal prismatic structure of the lowest triplet state (C_{2v} Symmetry). computed using the multi-state CASSCF/CASPT2 + RASSI approach, ANO-I basis, $\varepsilon_{\mathrm{IPEA}} = 0.25$ a.u.

Term (C_{2v})	Spin-Orbit Free	Spin-Orbit Coupled
1^3B_2	0.0	−0.1
		−0.1
		0.0
1^1A_1	7.7	7.7
1^1B_2	16.3	16.0
1^3A_1	21.1	21.1
		21.1
		21.3
2^1A_1	33.4	33.3
3^1A_1	38.0	37.9
2^3B_2	41.7	41.7
2^1B_2	49.8	49.9
4^1A_1	81.2	81.3

Table S11: DFT:BP86-optimized atomic coordinates of $[Mo(CN)_6]^{2-}$, singlet state (spin-restricted) (Å).

Mo	0.0000000	0.0000000	0.0000000
C	1.6192174	0.0000000	1.3424304
C	-0.8096087	1.4022834	1.3424304
C	1.6192174	0.0000000	-1.3424304
C	-0.8096087	1.4022834	-1.3424304
C	-0.8096087	-1.4022834	-1.3424304
C	-0.8096087	-1.4022834	1.3424304
N	2.5270741	0.0000000	2.0909924
N	-1.2635371	2.1885104	2.0909924
N	2.5270741	0.0000000	-2.0909924
N	-1.2635371	2.1885104	-2.0909924
N	-1.2635371	-2.1885104	-2.0909924
N	-1.2635371	-2.1885104	2.0909924

Table S12: DFT:BP86-optimized atomic coordinates of $[Mo(CN)_6]^{2-}$, singlet state (spin-unrestricted) (Å).

Mo	0.0340194	-0.0025839	0.0000000
C	0.7280715	-1.4788114	-1.3637018
C	0.8011545	1.4370042	-1.3611966
C	-1.5925981	0.0453336	-1.3205991
C	-1.5925981	0.0453336	1.3205991
C	0.7280715	-1.4788114	1.3637018
C	0.8011545	1.4370042	1.3611966
N	1.1665545	-2.2729113	-2.1115231
N	1.2797257	2.2084054	-2.1082621
N	-2.5084462	0.0703310	-2.0585861
N	-2.5084462	0.0703310	2.0585861
N	1.1665545	-2.2729113	2.1115231
N	1.2797257	2.2084054	2.1082621

Table S13: DFT:BP86-optimized atomic coordinates of $[Mo(CN)_6]^{2-}$, triplet state (Å).

Mo	0.0000000	0.0000000	-0.0864483
C	-1.3803847	1.5290262	-0.7060181
C	-1.2888760	0.0000000	1.5609974
C	-1.3803847	-1.5290262	-0.7060181
C	1.3803847	-1.5290262	-0.7060181
C	1.3803847	1.5290262	-0.7060181
C	1.2888760	0.0000000	1.5609974
N	-2.1259354	2.3161485	-1.1581560
N	-2.0163980	0.0000000	2.4846407
N	-2.1259354	-2.3161485	-1.1581560
N	2.1259354	-2.3161485	-1.1581560
N	2.1259354	2.3161485	-1.1581560
N	2.0163980	0.0000000	2.4846407

Table S14: DFT:BP86-optimized atomic coordinates of $[Mo(CN)_6]^{3-}$, quartet state (Å).

Mo	0.0000000	0.0000000	0.0000000
C	0.0000000	2.2357100	0.0000000
C	0.0000000	0.0000000	2.2357054
C	-2.2357109	0.0000000	0.0000000
C	0.0000000	-2.2357100	0.0000000
C	0.0000000	0.0000000	-2.2357054
C	2.2357109	0.0000000	0.0000000
N	0.0000000	3.4009693	0.0000000
N	0.0000000	0.0000000	3.4009641
N	-3.4009701	0.0000000	0.0000000
N	0.0000000	-3.4009693	0.0000000
N	0.0000000	0.0000000	-3.4009641
N	3.4009701	0.0000000	0.0000000

Table S15: DFT:BP86-optimized atomic coordinates of $[Mo(CN)_6]^{3-}$, doublet state (Å).

Mo	0.0000000	0.0000000	0.0000000
C	0.0000000	2.1936533	0.0000000
C	0.0000000	0.0000000	2.1936544
C	-2.1968955	0.0000000	0.0000000
C	0.0000000	-2.1936533	0.0000000
C	0.0000000	0.0000000	-2.1936544
C	2.1968955	0.0000000	0.0000000
N	0.0000000	3.3737511	0.0000000
N	0.0000000	0.0000000	3.3737523
N	-3.3766268	0.0000000	0.0000000
N	0.0000000	-3.3737511	0.0000000
N	0.0000000	0.0000000	-3.3737523
N	3.3766268	0.0000000	0.0000000

Table S16: DFT:BP86-optimized atomic coordinates of $[MoCl_6]^{2-}$, triplet state (Å).

Mo	0.0000000	0.0000000	0.0000000
Cl	0.0000000	0.0000000	2.4615332
Cl	2.4084425	0.0000000	0.0000000
Cl	0.0000000	-2.4084423	0.0000000
Cl	0.0000000	0.0000000	-2.4615332
Cl	-2.4084425	0.0000000	0.0000000
Cl	0.0000000	2.4084423	0.0000000

Table S17: DFT:BP86-optimized atomic coordinates of $[MoCl_6]^{2-}$, singlet state (spin-unrestricted) (Å).

Mo	0.0000000	0.0000000	0.0000000
Cl	0.0000000	0.0000000	2.4555665
Cl	2.4059523	0.0000000	0.0000000
Cl	0.0000000	-2.4059525	0.0000000
Cl	0.0000000	0.0000000	-2.4555665
Cl	-2.4059523	0.0000000	0.0000000
Cl	0.0000000	2.4059525	0.0000000

Table S18: Atomic coordinates (Å) of model shown in Figure S1.

Mo	12.590000	0.000000	0.000000
C	10.500060	0.000000	0.000000
N	9.363183	0.000000	0.000000
C	14.679940	0.000000	0.000000
N	15.816817	0.000000	0.000000
C	12.590000	-2.089940	0.000000
N	12.590000	-3.226817	0.000000
C	12.590000	2.089940	0.000000
N	12.590000	3.226817	0.000000
C	12.590000	-0.000000	-2.089940
N	12.590000	-0.000000	-3.226817
C	12.590000	0.000000	2.089940
N	12.590000	0.000000	3.226817
Mo	12.590000	6.295000	6.295000
C	10.500060	6.295000	6.295000
N	9.363183	6.295000	6.295000
C	14.679940	6.295000	6.295000
N	15.816817	6.295000	6.295000
C	12.590000	4.205060	6.295000
N	12.590000	3.068183	6.295000
C	12.590000	8.384940	6.295000
N	12.590000	9.521817	6.295000
C	12.590000	6.295000	4.205060
N	12.590000	6.295000	3.068183
C	12.590000	6.295000	8.384940
N	12.590000	6.295000	9.521817
O	12.590000	0.000000	6.295000
H	12.590000	0.950446	6.415069
H	12.590000	-0.121151	5.342675

Table S19: Z-matrix used to define twisted structures for the potential energy scan in Figure 2, main article. To obtain an initial structure with the twist angle θ, the parameter `dih4` should be set to $-\theta$.

```
zmat angstroms
mo
xx   1 xxmo2
 c    1 cmo3        2 cmoxx3
 c    1 cmo4        2 cmoxx4        3 dih4
 c    1 cmo5        2 cmoxx5        3 dih5
 c    1 cmo6        2 cmoxx6        3 dih6
 c    1 cmo7        2 cmoxx7        6 dih7
 c    1 cmo8        2 cmoxx8        6 dih8
 n    3 nc9         1 ncmo9         2 dih9
 n    4 nc10        1 ncmo10        2 dih10
 n    5 nc11        1 ncmo11        2 dih11
 n    6 nc12        1 ncmo12        2 dih12
 n    7 nc13        1 ncmo13        2 dih13
 n    8 nc14        1 ncmo14        2 dih14
variables
xxmo2       1.206662
cmo3        2.089999
cmoxx3       54.736
cmo4        2.089999
cmoxx4       54.736
dih4       -120.000
cmo5        2.089999
cmoxx5       54.736
dih5        120.000
cmo6        2.089999
cmoxx6      125.264
dih6        -60.000
cmo7        2.089999
cmoxx7      125.264
dih7       -120.000
cmo8        2.089999
cmoxx8      125.264
dih8        120.000
nc9         1.137000
ncmo9       180.000
dih9        180.000
nc10        1.137000
ncmo10      180.000
dih10       180.000
nc11        1.137000
ncmo11      180.000
dih11       180.000
nc12        1.137000
ncmo12      180.000
dih12       180.000
nc13        1.137000
ncmo13      180.000
dih13       180.000
nc14        1.137000
ncmo14      180.000
dih14       180.000
constants
end
```

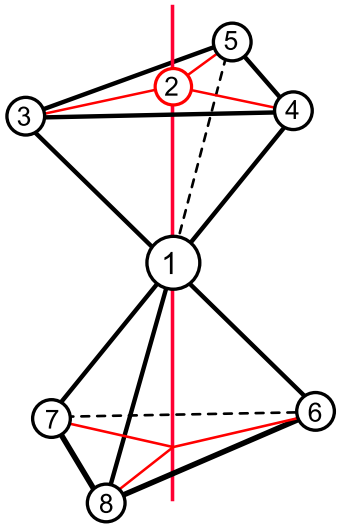

angle(3-1-2) = angle(4-1-2) = angle(5-1-2)
angle(6-1-2) = angle(7-1-2) = angle(8-1-2)
dih(3-2-1-6) = dih(4-2-1-7) = dih(5-2-1-8) = $-\theta$

Figure S8: Definitions of geometric constraints applied to generate the potential energy scan along the Bailar twist coordinate θ (Figure 2, main article). Atom 1 is Mo, 2 is a dummy atom lying in the center of triangle 2-3-4, atoms 3–8 are carbons. In spin restricted calculations for the singlet state the following constraints were also applied: angle(3-2-4) = angle(4-2-5) = angle(3-2-5) and angle(6-2-7) = angle(7-2-8) = angle(6-2-8) in addition to the constrains given above; this was necessary to avoid a significant deformation of the structure for $\theta > 45°$, whose occurrence would prevent an interpretation of the resulting structures as close to the octahedral one.

Table S20: Comparison of calculated and experimental ν_{CN} bands active in IR and Raman spectroscopy.

Calcd Octahedral[a]			Calcd Prismatic[b]			Exptl[c]
S(R)	S(U)	T	S(R)	S(U)	T	
IR:						
2022 (e_u, 16%)	2062(a_{2u}, 19%)	2074(a_{2u}, 15%)	2072(e', 100%)	2073(a'', 2%)	2075(b_1, 2%)	2088
2104(a_{2u}, 100%)	2071(e_u, 100%)	2080(e_u, 100%)	2072(a''_2, 28%)	2075(a', 72%)	2080(a_1, 43%)	
				2082(a', 100%)	2098(b_1, 100%)	
				2087(a'', 3%)	2108(a_1, 11%)	
				2099(a', 57%)		
Raman:						
2035(b_{1g}, 92%)	2072(a_{1g}, 85%)	2083(a_{1g}, 84%)	2072(e', 18%)	2073(a'', 16%)	2075(b_1, 19%)	2094($\sim$ 50%)
2057(a_{1g}, 100%)	2078(b_{1g}, 59%)	2087(b_{1g}, 73%)	2079(e'', 48%)	2075(a', 19%)	2080(a_1, 24%)	2106 (100%)
2110(a_{1g}, 72%)	2087(a_{1g}, 100%)	2094(a_{1g}, 100%)	2104(a'_1, 100%)	2082(a', 25%)	2095(b_2, 20%)	
				2087(a'', 26%)	2098(b_1, 16%)	
				2091(a'', 47%)	2103(a_2, 48%)	
				2099(a', 100%)	2108(a_1, 100%)	

[a]Real symmetry is not O_h, but D_{4h} due to uneven occupation of the t_{2g} orbitals. [b]Symmetry is D_{4h} for S(R), C_s for S(U), C_{2v} for T. [c]From ref. 6. Abbreviations: S – singlet, T – triplet, (R)/(U) – restricted/unrestricted description. All values in cm^{-1} at BP86/def2-TZVP level. Symmetry irrep and relative intensity with respect to the most intense computed transition in parentheses.

Comments to Table S20.

The experimental IR and Raman data are taken from ref. 6. Theoretical data were computed for the octahedral and trigonal prismatic structures, assuming either triplet or singlet state (the latter can be treated using either restricted or unrestricted approach). Concerning the number of allowed bands for the octahedral structure, one should remember that the actual symmetry is D_{4h} due to uneven occupation of the t_{2g} orbitals. Therefore, the actual number of ν_{CN} bands active in IR / Raman is: 2 / 3 (and not 1 / 2, as might be inferred from the ideal O_h symmetry) Likewise, the prismatic structure has the D_{3h} symmetry only in spin-restricted calculations for the singlet state, but it has instead, the C_{2v} symmetry for the triplet or the C_s symmetry for the singlet in spin-unrestricted calculations. This symmetry lowering (to C_s) for the unrestricted singlet results is clearly an artifact of the unrestricted approach: the energy is improved (compared to closed-shell singlet), but the structure and thus frequencies not necessarily so. The singlet structure obtained from spin-restricted calculations also results in a lower CASPT2 energy, confirming that this more symmetric structure is closer to the CASPT2 energy miniumum, and presumably to the real structure of the singlet state.

IR spectrum

The fact that the experimental spectrum contains only one ν_{CN} band is best reproduced by the results from (restricted) singlet-state calculations for the trigonal prism geometry. Although for D_{3h} symmetry there should be two IR-active modes (a_2'', e'), they accidentally overlap up to < 1 cm^{-1}! For all other structures there are at least two IR-active ν_{CN} modes separated by at least 5 cm^{-1}. However, given that the FWHM of the experimental ν_{CN} band is ~ 15 cm^{-1}, the results calculated for the triplet octahedral structure (two bands separated by only 6 cm^{-1}) may also be in an acceptable agreement with the experimental IR spectrum.

Raman spectrum

For none of the structures the computed results are in perfect agreement with the experimental spectrum (where two ν_{CN} bands are observed). The best agreement seems to be obtained, again, for the octahedral structure in the triplet state and for the trigonal prism structure in the (restricted) singlet state. We note that all the results, including these two, predict a higher number of allowed ν_{CN} bands than actually appear in the Raman spectrum but this can be probably explained by band overlapping. Particularly the results from (restricted) singlet calculations for the trigonal prism geometry give a reasonable distribution of the two more intense bands; the only problem is with the lowest, less intense band which is not observed although its computed relative intensity is 18% of the most intense band.

In conclusion, the results of the analysis for the present case are not conclusive due to band overlapping. They do not rule out, but neither fully confirm, the possibility of a trigonal prismatic geometry.

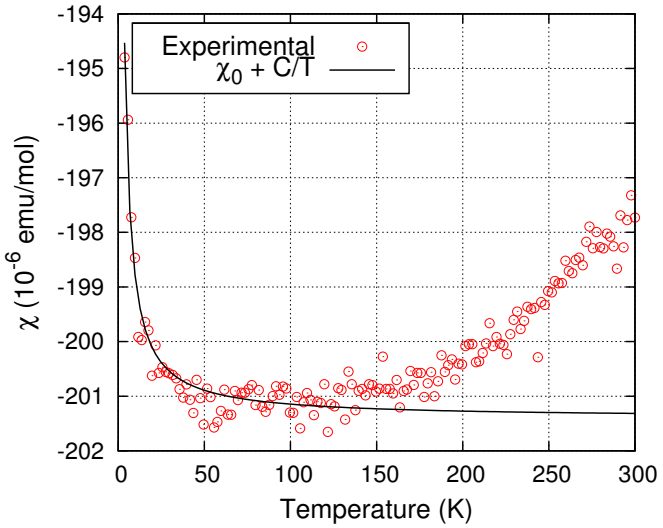

Figure S9: Temperature dependence of molar magnetic susceptibility of **1** χ measured on the SQUID magnetometer. A trace of paramagnetism appears at very low temperatures (which is attributed to a contamination of the sample by ubiquitous iron at very low concentration); moreover, there is an unexpected increase of χ for higher temperatures (attributed to increasing a Boltzmann population of the higher-energy paramagnetic states). A function of form: $\chi_0 + C/T$ was fitted to the experimental data for $T < 150K$, yielding: $\chi_0 = -201.4 \cdot 10^{-6}$ emu/mol, $C = 25.42 \cdot 10^{-6}$ emu·K/mol.

Thermodynamical model to explain the temperature dependence of magnetic susceptibility for a system with close lying singlet and triplet states

Let us consider a two-level system, with a singlet ground state and an excited triplet state (at the energy $\Delta > 0$ above the singlet). When the system is placed in the external magnetic field B at finite temperature T, the canonical partition function reads:

$$Z = 1 + e^{-y} \sum_{m=-1}^{1} e^{xm},$$

with $m = -1, 0, 1$ – the magnetic quantum number in the triplet state; the dimensionless, positive quantities $x := g\beta/(kT)$, $y := \Delta/(kT)$; $g \approx 2$ – the electron's gyromagnetic ratio; β – the Bohr magneton; k – the Boltzmann constant. The average value of the magnetic quantum number reads:

$$\langle m \rangle = Z^{-1} e^{-y} \sum_{m=-1}^{1} m e^{xm} = \frac{e^{-y}(e^{x} - e^{-x})}{1 + e^{-y}(e^{x} + e^{-x} + 1)} =: m(x, y), \tag{S1}$$

from which the magnetization per mole can be calculated:

$$M = Ng\beta\langle m \rangle = N_A g\beta m(x, y),$$

where N is the Avogadro constant. The molar magnetic susceptibility reads:

$$\chi = \frac{\partial M}{\partial B} = Ng\beta \frac{\partial m}{\partial B} = Ng\beta \cdot \frac{\partial m}{\partial x} \cdot \frac{g\beta}{kT} = \frac{N(g\beta)^2}{kT} \cdot \frac{\partial m}{\partial x}.$$

In the regime of weak fields: $kT \gg g\beta B$, i.e., $x \ll 1$, the function in eq. (S1) reduces to

$$m(x, y) = \frac{2xe^{-y}}{1 + 3e^{-y}} = \frac{2x}{3 + e^{y}}$$

and we have simply:

$$\chi = N\frac{(g\beta)^2}{kT}\cdot\frac{2}{3+e^y} = \frac{2(g\beta)^2}{3k}\cdot\frac{1}{T}\cdot\frac{1}{1+\frac{1}{3}e^y}. \tag{S2}$$

So far we neglected the effect of spin-orbit coupling. This effect can be introduced approximately by invoking now that, due to the spin-orbit coupling, the effective magnetic moment of the triplet state differs from its spin-only value. Thus, effectively, the g factor in (S2) needs to be modified by introducing an *ad hoc* parameter a in the following way: $g = 2\sqrt{a}$; the unit value of a would correspond to the situation without the spin-orbit coupling. Having done this conjecture, the susceptibility reads

$$\chi = \frac{8N\beta^2}{3k}\cdot\frac{a}{T}\cdot\frac{1}{1+\frac{1}{3}e^y}.$$

Taking into account that in the CGS units the first factor is (approximately) 1 emu·K/mol, we have the following final formula:

$$\chi(T) = \frac{a}{T}\cdot\frac{1}{1+\frac{1}{3}e^{\frac{\Delta}{kT}}} =: f(T), \tag{S3}$$

which was used in the text as eq. (1).

It is worth to note that if Δ was equal to 0 (i.e., the singlet and the triplet were degenerate), the equation (S3) would reduce to 75% of the triplet susceptibility (a/T, in the CGS units). This is a correct limiting value because, if the singlet and triplet state were degenerated, 75% of the centers would be in the triplet and 25% in the singlet state, due to the statistics.